

The electronic band-structures of the superlattices  $(\text{Ga}_{0.47}\text{In}_{0.53}\text{As})_m/(\text{InP})_m$  (110) with  $m = 1-25$

This article has been downloaded from IOPscience. Please scroll down to see the full text article.

1989 J. Phys.: Condens. Matter 1 8263

(<http://iopscience.iop.org/0953-8984/1/43/027>)

View [the table of contents for this issue](#), or go to the [journal homepage](#) for more

Download details:

IP Address: 171.66.16.96

The article was downloaded on 10/05/2010 at 20:45

Please note that [terms and conditions apply](#).

## LETTER TO THE EDITOR

# The electronic band-structures of the superlattices (Ga<sub>0.47</sub>In<sub>0.53</sub>As)<sub>m</sub>/(InP)<sub>m</sub> (110) with $m = 1-25$

Zhizhong Xu

Surface Physics Laboratory, Fudan University, Shanghai, People's Republic of China

Received 11 July 1989

**Abstract.** The electronic band-structures of lattice-matched superlattices (Ga<sub>0.47</sub>In<sub>0.53</sub>As)<sub>m</sub>/(InP)<sub>m</sub> (110) with  $m = 1-25$  were calculated by the renormalisation approach in a tight-binding frame. The transitions of the electronic characters from three-dimensional to two-dimensional with increasing superlattice layer number are discussed. It is pointed out that the valence band dispersions of superlattices both along the directions parallel and normal to the superlattice planes show non-parabolic features.

In order to examine how the electronic characters change from three-dimensional to two-dimensional with increasing layer number of superlattices and, on the other hand, to study the electronic structures of superlattices Ga<sub>0.47</sub>In<sub>0.53</sub>As/InP, which have potential for a wide range of applications in the photoelectronics industry, we have calculated the electronic band structures of lattice-matched superlattices (Ga<sub>0.47</sub>In<sub>0.53</sub>As)<sub>m</sub>/(InP)<sub>m</sub> (110) with  $m = 1-25$  by using the renormalisation technique in a tight-binding frame (Graft *et al* 1987). The tight-binding parameters given by Vogl *et al* (1983) were adopted. The virtual crystal approximation with a non-linear correction (Mbaye and Verie 1984) was applied to the alloy Ga<sub>0.47</sub>In<sub>0.53</sub>As. The value of the valence band discontinuity for the Ga<sub>0.47</sub>In<sub>0.53</sub>As/InP interface is estimated with Harrison's formula (Harrison 1980) to be  $\Delta E_v = 0.28$  eV.

The conduction band dispersions along the [110] direction (normal to the superlattice plane) and the [1 $\bar{1}$ 0] direction (parallel to the superlattice plane) are shown in figure 1. For the [110] direction, the unit of wavevector  $K_{[110]}$  is  $L^{-1}$ , where  $L$  is the period length of the superlattice in the [110] direction. For the [1 $\bar{1}$ 0] direction, the unit of wavevector  $K_{[1\bar{1}0]}$  is  $\text{\AA}^{-1}$ . From figure 1, it can be observed that the conduction band dispersion curves along the [110] direction become more even as the layer number of the superlattice increases. The total widths of conduction bands along the [110] direction for  $m = 1, 5, 10, 15, 20, 25$  are listed in the third row of table 1. When  $m = 25$ , the width of conduction band along the [110] direction reduces to 4 meV, and the conduction band along [110] direction actually turns into an energy level. This means that the conduction-band electrons show distinct two-dimensional character as the layer number  $m$  reaches 25 (the period length reaches 103.7  $\text{\AA}$ ). On the other hand, in the [1 $\bar{1}$ 0] direction, the conduction-band dispersions show a tendency to slow growth as the layer number increases. The fourth row of table 1 shows the average curvatures of conduction band curves in the range of  $K_{[1\bar{1}0]} = 0-0.045 \text{\AA}^{-1}$  (about 6% of the reduced Brillouin zone (BZ) in the [1 $\bar{1}$ 0] direction). Here the curvatures are the relative values taking the curvature for  $m = 1$  as

1. In addition, we find that in the range of  $K_{[1\bar{1}0]} = 0-0.01 \text{ \AA}^{-1}$  (about 1.3% of the reduced BZ in the  $[1\bar{1}0]$  direction) all the conduction-band curves show parabolic features. This may predict that the electronic states of the conduction bands of the superlattices  $(\text{Ga}_{0.47}\text{In}_{0.53}\text{As})_m/(\text{InP})_m$  (110) can be studied using an envelope-function approach based on the effective-mass approximation.

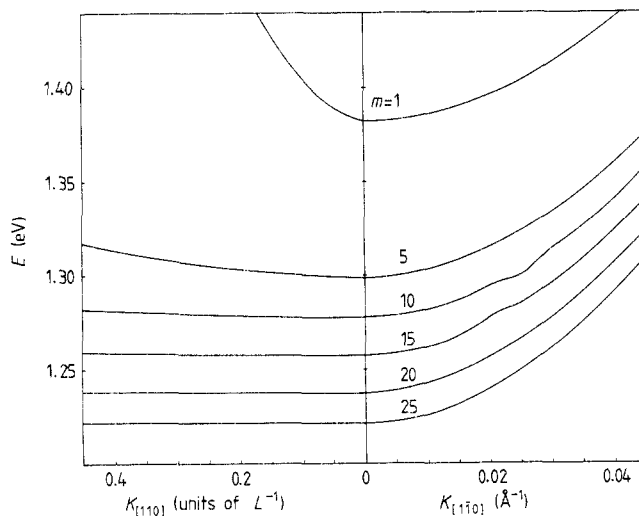


**Figure 1.** The band dispersions near the bottom of the conduction band along the  $[110]$  and  $[1\bar{1}0]$  directions for layer numbers  $m$ . In the  $[110]$  direction the unit of wavevector  $K_{[110]}$  is  $L^{-1}$ , where  $L$  is the period length of  $(\text{Ga}_{0.47}\text{In}_{0.53}\text{As})_m/(\text{InP})_m$  along the  $[110]$  direction and  $L = 10.6m/\sqrt{6} \text{ \AA}$ .

**Table 1.** The variation width of the conduction band along the  $[110]$  direction and the average curvature of the conduction band curve along the  $[110]$  direction with layer number for the lattice matched superlattices  $(\text{Ga}_{0.47}\text{In}_{0.53}\text{As})_m/(\text{InP})_m$ .

Layer number $m$	1	5	10	15	20	25
Period length $L$ ( $\text{\AA}$ )	4.15	20.74	41.48	62.22	82.96	103.70
Band width $W_c$ (eV)	1.029	0.434	0.123	0.040	0.013	0.004
Average curvature	1.0	1.09	1.13	1.17	1.20	1.22

Figure 2 shows the electronic effective mass at the bottom of conduction bands ( $\Gamma$ -point) along the  $[110]$  and  $[1\bar{1}0]$  directions as a function of the layer number of the superlattices. The longitudinal electronic effective mass  $m_{[110]}^*$  grows quickly with increasing layer number but the transverse electronic effective mass  $m_{[1\bar{1}0]}^*$  decreases slowly with increasing layer number. (In figure 2,  $m_0$  denotes the mass of a static electron.) The ratio of the longitudinal effective mass to the transverse effective mass

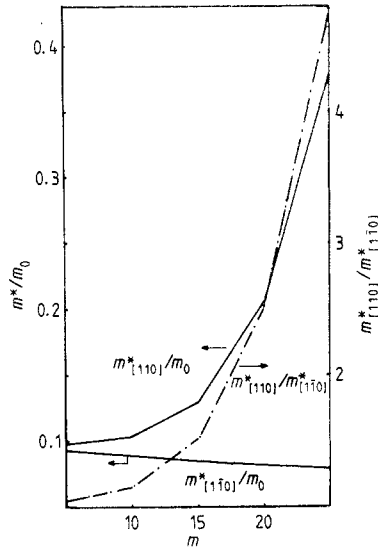


**Figure 2.** The electronic effective mass at the bottom of the conduction band along the [110] and [110] directions as a function of the layer number of the superlattice.

$m_{[110]}^*/m_{[110]}^*$  as a function of layer number is also shown in figure 2. It can be observed from figure 2 that the rate  $m_{[110]}^*/m_{[110]}^*$  shows a tendency to rapid increase with increasing layer number. At  $m = 25$ ,  $m_{[110]}^*/m_{[110]}^* = 4.71$  and the electronic transport properties will thus show approximately two-dimensional characteristics.

The valence band dispersions for  $m = 1$  and  $m = 5$  are shown in figures 3 and 4 respectively. The dispersion curves near the top of valence band exhibit a large non-parabolic feature. When using the effective-mass approximation, O'Reilly and Witchlow (1986) discussed the dispersions near the top of valence band in the quantum wells and pointed out that the valence bands of these quantum wells showed very complicated structures due to strong interactions between the heavy- and light-hole subbands. Using the pseudopotential approach, Ninno *et al* (1987) discussed the band dispersions near the top of valence band in the superlattice plane for  $(\text{Ga}_{0.47}\text{In}_{0.53}\text{As})_m/(\text{InP})_m$  (001) and obtained the similar result that the dispersion curves near the top of valence band along the transverse direction (parallel to the superlattice plane) showed a large non-parabolic feature. Our calculated results indicate that the valence-band dispersions near the top are non-parabolic not only for the transverse direction but also for the longitudinal direction (normal to the superlattice plane). Moreover, along the transverse direction the valence-band dispersions show stronger non-parabolicities for  $m = 5$  than for  $m = 1$ , but along the longitudinal direction they show the converse. This implies that for the transverse direction the non-parabolicities of the valence bands grow with increasing layer number and for the longitudinal direction they decrease with increasing layer number. We may imagine that with increasing layer number the valence bands in the longitudinal direction become more and more level, so that their nonparabolicities in this direction are indistinct.

The energy at the bottom of the conduction band, the energy at the top of the valence band and the width of forbidden gap are given in figure 5 as a function of the layer thickness. Here the energy at the top of the valence band of the semiconductor InP is taken to be the zero-point of the ordinate. It can be observed from figure 5 that the width of forbidden gap decreases with the increase of layer number.

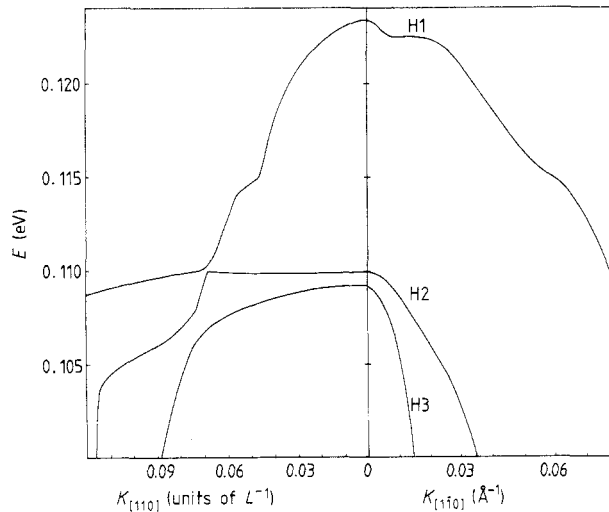


**Figure 3.** The band dispersions near the top of the valence band along the [110] and  $\bar{1}\bar{1}0$  directions for the monolayer superlattice  $\text{Ga}_{0.47}\text{In}_{0.53}\text{As}/\text{InP}$  ( $m = 1$ ). In the [110] direction the unit of the wavevector  $K_{[110]}$  is  $L^{-1}$ , where  $L$  is the period length of the superlattice along the [110] direction and  $L = 4.15 \text{ \AA}$ .

To examine how the electronic characteristics of the superlattices change from three-dimensional to two-dimensional, we take the  $\text{Ga}_{0.47}\text{In}_{0.53}\text{As}$  alloy layers in the superlattice as the quantum wells and suppose that the electrons in each well cannot pass through the barrier even approximately (i.e. assuming that the width of barrier is infinite). Then every well may be regarded as a single well and we can calculate the energy levels on the basis of the single quantum-well model using simple formulae. The parameters adopted in this calculation, including the widths of forbidden gaps of the  $\text{Ga}_{0.47}\text{In}_{0.53}\text{As}$  alloy and the semiconductor InP and the electronic effective mass of the alloy ( $E_{\text{g}}^{\text{alloy}}$ ,  $E_{\text{g}}^{\text{InP}}$  and  $m_{\text{alloy}}^*$ ) are obtained with the same tight-binding parameters given by Vogl *et al* (1983) and the values of these parameters are given as  $E_{\text{g}}^{\text{alloy}} = 0.87 \text{ eV}$ ,  $E_{\text{g}}^{\text{InP}} = 1.41 \text{ eV}$ , and  $m_{\text{alloy}}^* = 0.067 m_0$  (Xu 1986). With these parameters and the valence band discontinuity  $\Delta E_{\text{v}} = 0.28 \text{ eV}$ , the height of barrier for the conduction band electrons is calculated to be  $U = 0.026 \text{ eV}$ . The calculated results are listed in table 2. The lowest energy level of the quantum well  $E_{\text{w}}$  and the energy at the bottom of the conduction band  $E_{\text{c}}$  are given in the second and the third rows of table 2 separately. In the fourth row the difference  $\Delta = E_{\text{w}} - E_{\text{c}}$  is listed. In order to test the validity of the assumption that the width of the barrier is infinite, the tunnelling probability of the electrons in the quantum well through the barrier, the width of which is determined by the layer number of the superlattice, is also calculated and the results are listed in the fifth row of table 2. At  $m = 25$ , the tunnelling probability is reduced to 0.3% and each well may be assumed to be approximately independent. From table 2, it can be seen that the energy level  $E_{\text{w}}$  calculated on the basis of the single-well model is very close to the energy at the bottom of the conduction band  $E_{\text{c}}$  (the difference  $\Delta$  is only about 0.01 eV) when  $m = 25$ . Table 1 also shows that at  $m = 25$  the band width along the [110] direction (normal to the superlattice plane)  $\Delta W_{\text{c}}$  is reduced to 0.004 eV, which can be regarded as an energy level (not a band). So, when  $m = 25$  the superlattice can be treated as a multi-quantum-well (MQW) system.

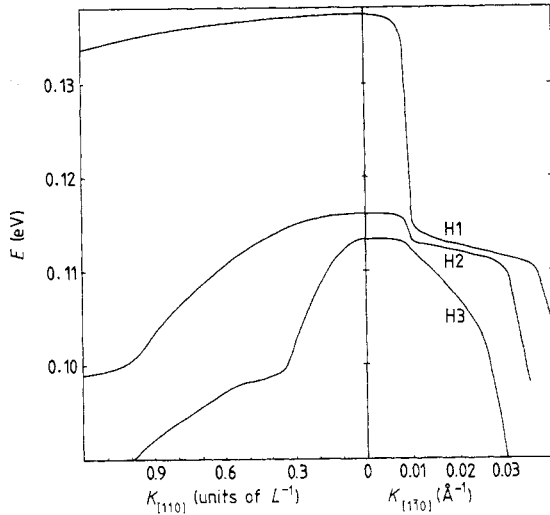


**Figure 4.** The band dispersions near the top of the valence band along the [110] and  $[1\bar{1}0]$  directions for the superlattice  $(\text{Ga}_{0.47}\text{In}_{0.53}\text{As})_5/(\text{InP})_5$  ( $m = 5$ ). In the [110] direction the unit of the wavevector  $K_{[110]}$  is  $L^{-1}$ , where  $L$  is the period length of superlattice along the [110] direction and  $L = 20.74 \text{ \AA}$ .

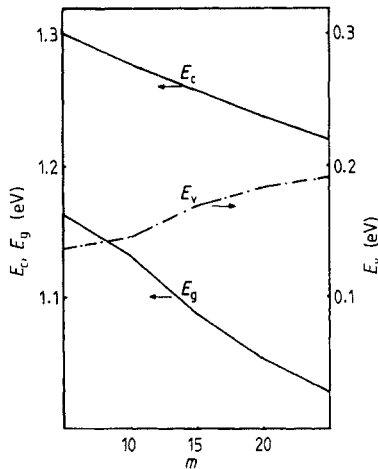


**Figure 5.** The energy at the bottom of the conduction band  $E_c$ , the energy at the top of the valence band  $E_v$  and the width of the forbidden gap  $E_g$  as a function of the layer number with the origin of energies taken to be the top of the valence band of the semiconductor InP.

**Table 2.** The lowest energy level in the quantum well  $E_w$ , the energy at the bottom of the conduction band  $E_c$  and the tunnelling probability through the barrier (with finite width) for the electrons in the well D.

Layer number $m$	5	10	15	20	25
$E_w$ (eV)	1.380	1.331	1.286	1.254	1.231
$E_c$ (eV)	1.299	1.278	1.258	1.238	1.221
$\Delta = E_w - E_c$	0.081	0.053	0.028	0.016	0.010
$D$	0.512	0.212	0.054	0.013	0.003

In conclusion, with increasing layer number of the superlattice the energy band in the direction normal to the superlattice plane gradually becomes an energy level and the ratio of the longitudinal effective mass to the transverse effective mass  $m_{[110]}^*/m_{[11\bar{1}0]}^*$  increases rapidly. These facts mean that the electronic properties in the superlattice are changing from three-dimensional to two-dimensional. Moreover, as the layer number of the superlattice increases, the tunnelling probability of electrons in the quantum wells through the barriers reduces progressively and the superlattice gradually becomes a MQW system. On the other hand, the valence band dispersions display considerable non-parabolic features both for the transverse and longitudinal directions. For the transverse direction the non-parabolicities grow with increasing superlattice layer number and for the longitudinal direction they decrease.

This work was supported by Chinese Natural Science Foundation.

### References

- Graft R D, Lohrmann D J, Parravicina G P and Resca L 1986 *Phys. Rev. B* **36** 4782  
Harrison W A 1980 *Electronic Structures and the Properties of Solids* (New York: Freeman)  
Mbaye A A and Verie C 1984 *Phys. Rev. B* **29** 3756  
Ninno D, Hagon J P and Jaros M 1987 *Semicond. Sci. Technol.* **2** 261  
O'Reilly E P and Witchlow 1986 *Phys. Rev. B* **34** 6030  
Vogl P, Hjalmarson H P and Dow J D 1983 *J. Phys. Chem. Solids* **44** 365  
Xu Zhizhong 1986 *Chinese J. Semicond.* **7** 665